Efficacy of positron emission tomography / computed tomography (PET/CT) fusion imaging in diagnosis of different types of lung cancer

Essay
Submitted for partial fulfillment of Master degree in Radiodiagnosis

By: Chrestin Haroun Kaisar M.B.B.Ch.

Supervised by

Dr. /Annie Mohamed Nasr Eldin

Professor of Radiodiagnosis
Faculty of medicine
Ain shams university

Dr. / Sherine Ibrahim Sharara

Lecturer of Radiodiagnosis
Faculty of medicine
Ain shams university
2010

كفاءة التصوير بالأشعة المقطعية مع الإنبعاث البوزيتروني في تشخيص انواع سرطان الرئة المختلفة

رسالة مقدمه من كرستين هارون قيصر سعد بكالوريوس الطب والجراحة كلية الطب عين شمس

توطئة للحصول على درجة الماجستير في الأشعة التشخيصية

تحت إشراف

د/ أنى محمد نصر الدين أستاذ الأشعة التشخيصية كلية الطب جامعة عين شمس

د/ شيرين ابراهيم شراره مدرس الأشعة التشخيصية كلية الطب جامعة عين شمس

Introduction

Cancer is one of the leading causes of morbidity and mortality even in developed countries. Complex clinical decisions about treatment of tumors are largely guided by imaging findings, among other factors. Most radiological procedures map the anatomy and morphology of tumors with little or no information about their metabolism (*Kapoor et al., 2004*).

Lung cancer is a common disease with approximately 3 million new cases per year worldwide and is the leading cause of cancer related death in many countries. Eighty percent of the lung cancers are non small cell lung cancers (NSCLC) and 20% are small cell lung cancers (SCLC). Staging a patient with lung cancer implies an accurate determination of the size of the tumor, the potential infiltration of the tumor into the adjacent structures, the involvement of hilar and mediastinal lymph nodes and the detection of distant metastasis (Wever et al., 2007).

The most important prognostic indicator in lung cancer is the extent of disease. The Union Internationale Contre le Cancer (UICC) and the American Joint Committee for Cancer Staging (AJCC) have developed the tumor, node, and metastasis (TNM) staging system, which takes into account the degree of

١

spread of the primary tumor, the extent of regional lymph node involvement, and the presence or absence of distant metastasis (*Hassan*, 2009).

CT is the imaging modality of choice to define the extent of the primary tumor and to assess the tumor involvement of the pleural surfaces and the thoracic wall. Mediastinoscopy, CT and MRI are being used for assessing the involvement of lymph nodes. The main limitation of CT and MRI is using a size criterion of 1 cm for the diagnosis of tumor involvement (*kumar et al.*, 2010).

Positron emission computed tomography (PET) is a functional diagnostic imaging technique, which can accurately measure in vivo distribution of a variety of radiopharmaceuticals. The ability of PET to study various biological processes (glucose, amino acid, phospholipids, receptors etc.) opens up new possibilities for both day to day clinical use and research applications in the practice of oncology. The role of PET has been already established in initial staging, monitoring the response to the therapy and recurrence detection of various important cancers (kumar et al., 2010).

Previous studies have demonstrated that PET is more accurate than computed tomography (CT) for the diagnosis and staging of NSCLC. The main disadvantage of PET is the poor quality of the anatomic information. To overcome this disadvantage of PET, new imaging systems using integrated PET/CT were developed recently (Kanzakia et al., 2010).

PET/CT has been introduced into the diagnostic algorithms for oncologic patients because they provide valuable functional information. The hybrid PET/CT technique acquires both anatomic (CT) and metabolic (PET) images in a single session, combining the benefits of each modality and minimizing their limitations (*Pinilla and Gómez*, 2009).

PET/CT has a very high sensitivity and a high negative predictive value for lesion detection as compared to conventional morphological modalities like Computed Tomography (CT), Ultrasonography (US) and Magnetic Resonance Imaging (MRI). Recent data show that PET/CT has higher sensitivity and specificity as compared to PET and CT alone as it provides better characterization and localization of lesion (*Kumar et al.*, 2010).

In conclusion, PET/CT scanning is a combination of PET and CT that generates precise co-registered functional and structural images, that is positioned to reduce the false positive and negative mis-diagnoses of single CT or PET scan (*Bao-jun et al.*, 2009).

Aim Of The Work

To evaluate the role of fused PET/CT images in diagnosis and staging of patients with lung cancer hoping to reach an effective treatment.

ANATOMY

Pleura

The pleura is a serous membrane that covers the lung (the visceral pleura) and lines the thoracic cavity and mediastinum (the parietal pleura). Parts of the pleura are named according to the site, for example costal, diaphragmatic, mediastinal and apical pleura. The visceral and parietal layers are continuous with each other anterior and posterior to lung roots but below the hilum the two layers hang down in a loose fold called the pulmonary ligament. This may extend to the diaphragm or have a free inferior border and allows descent of lung root in respiration and also distension of the pulmonary veins (Stephanie et al., 2004).

The visceral pleura extends into interlobar and accessory fissures. At rest, the parietal pleura extends deeper into the costophrenic and costomediastinal recesses than do the lung and visceral pleura (Stephanie et al., 2004).

	Visceral pleura	Parietal pleura
Anterior	6 th costal cartilage	6 th costal cartilage
Mid-axillary	8 th rib	10 th rib
Posterior	T_{10}	T_{12}

Table (1): Lower limits of the lung and pleura (Stephanie et al., 2004).

The parietal pleura is supplied by the systemic vessels. The visceral pleura receives arterial supply from both the bronchial and the pulmonary circulation (Stephanie et al., 2004).

Anatomy of the lung

Each lung is conical in shape and has an apex, base, three borders and two surfaces. The surfaces are costal and mediastinal surfaces. The borders are inferior, posterior and anterior borders (*Goerres et al.*, 2002).

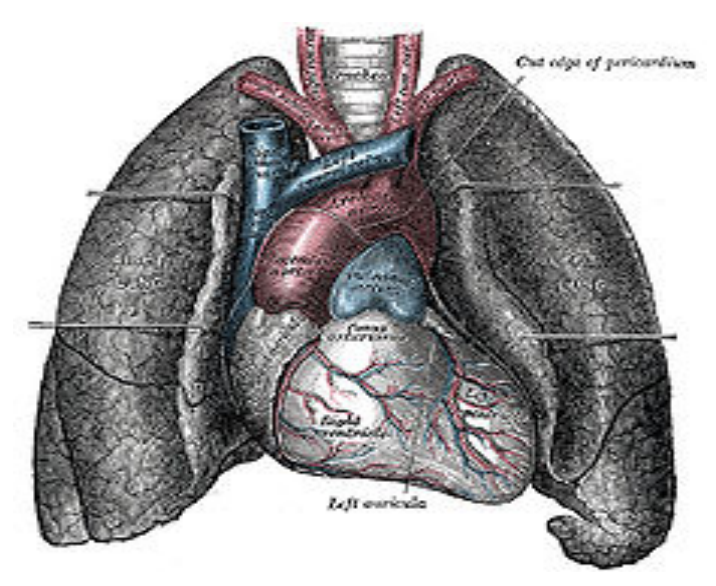


Fig. (1): Anatomy of the lung (Standring, 2005).

Apex:

Is the rounded upper extremity protruding above the thoracic inlet. The apex rises 3-4 cm above the level of the

first costal cartilage although it levels posteriorly with the neck of the first rib (David et al., 2005).

Base

It is semilunar and concave, and rests upon the superior surface of the diaphragm, which separates the right lung from the right lobe of the liver and the left lung from the left lobe of the liver, the gastric fundus and spleen (David et al., 2005).

The costal surface

The costal surface of the lung is smooth and convex, and its shape is adapted to that of the thoracic wall, which is vertically deeper posteriorly. It is in contact with the costal pleura and exhibits, in specimens, grooves that correspond with the overlying ribs (*David et al.*, 2005).

The medial surface

It has a posterior vertebral and anterior mediastinal parts. The vertebral part lies in contact with the sides of the thoracic vertebrae and intervertebral discs. The mediastinal area is deeply concave, because it is adapted to the heart at the cardiac impression, which is much larger and deeper on the left lung (*David et al.*, 2005).

The Inferior border

It is thin and sharp where it separates the base from the costal surface and extends into the costo-diaphragmatic recess. It is more rounded medially where it separates the base from the mediastinal surface (*David et al.*, 2005).

The posterior border

It corresponds to the heads of the ribs. It has no recognizable markings and is really a rounded junction of costal and vertebral (medial) surfaces (*David et al.*, 2005).

The anterior border

The thin and sharp anterior border overlaps the pericardium. On the right it corresponds closely to the costo-mediastinal line of pleural reflection, and is almost vertical. On the left it approaches the same line above; however, below the fourth costal cartilage it shows a variable cardiac notch (*David et al.*, 2005).

Other impressions of the lung surface

In addition to these pulmonary features, preserved lungs show a number of other impressions that indicate their relations with surrounding structures (*David et al.*, 2005).

On the right lung (Fig.2), the cardiac impression is related to the anterior surface of the right auricle, the antero-lateral surface of the right atrium and partially to the anterior surface of the right ventricle. This impression ascends anterior to the hilum as a wide groove for the superior vena cava and the end of the right brachiocephalic vein. Posteriorly this groove is joined by a deep sulcus which arches forwards above the hilum and is occupied by the azygos vein (*David et al.*, 2005).

The right side of the oesophagus makes a shallow vertical groove behind the hilum and the pulmonary ligament. Postero-inferiorly the cardiac impression is confluent with a short wide groove adapted to the inferior vena cava (*David et al.*, 2005).

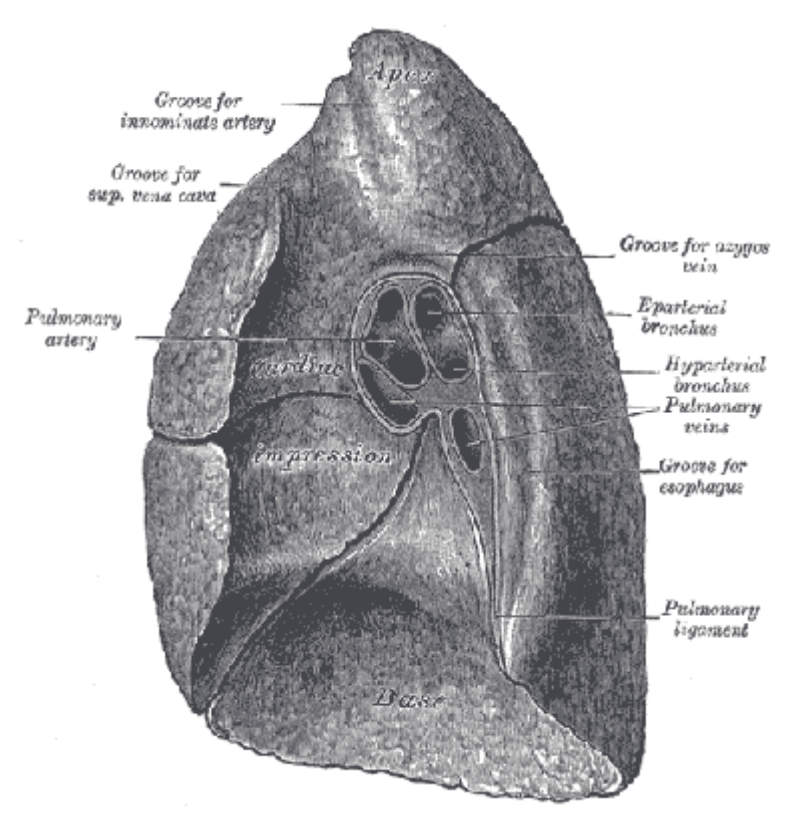


Fig. (2): Mediastinal surface of right lung (Standring, 2005).

On the left lung (Fig.3), the cardiac impression is related to the anterior and lateral surfaces of the left ventricle and auricle. A large groove arches over the hilum, and descends behind it and the pulmonary ligament, corresponding to the aortic arch and descending aorta. From its summit a narrower groove ascends to the apex for

the left subclavian artery. In front of the subclavian groove there is a faint linear depression for the left brachiocephalic vein (*David et al.*, 2005).

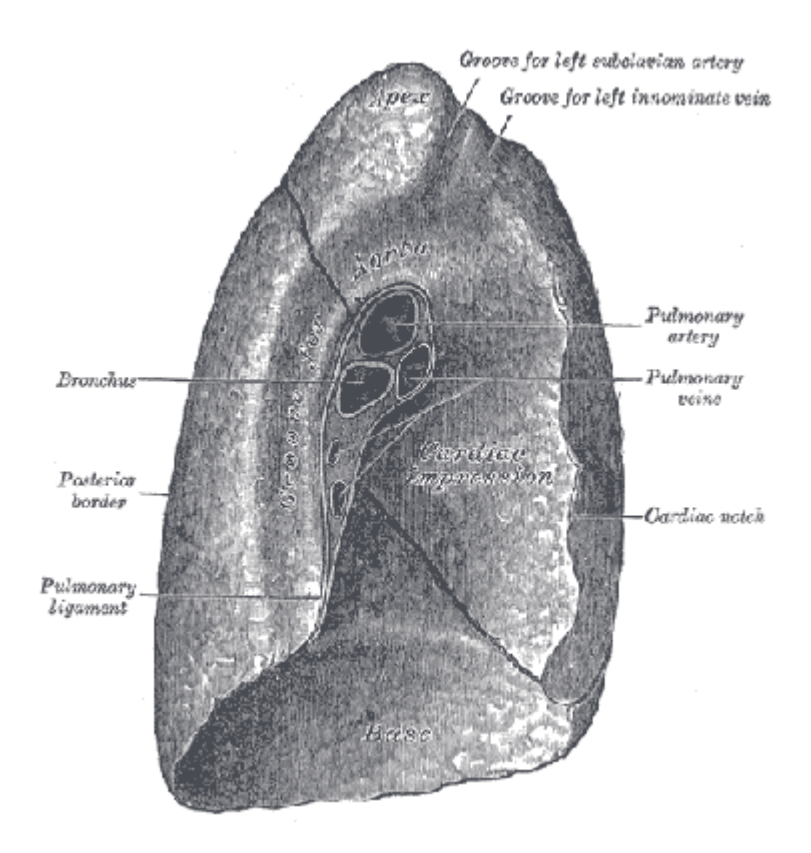


Fig. (3): Mediastinal surface of left lung (Standring, 2005).

Pulmonary hila

The pulmonary root lies opposite the bodies of the fifth to seventh thoracic vertebrae and connects the medial surface of the lung to the heart and trachea. It is formed by a group of structures that enter or leave the hilum. These

are the principal bronchus, pulmonary artery, two pulmonary veins, bronchial vessels, a pulmonary autonomic plexus, lymph vessels, bronchopulmonary lymph nodes and loose connective tissue, which are all enveloped by pleura (*David et al.*, 2005).

The root of the right lung lies behind the superior vena cava and part of the right atrium, and below the azygos vein (*Goerres et al., 2002*). The sequence from above downwards is superior lobar bronchus, pulmonary artery, principal bronchus and lower pulmonary vein (*David et al., 2005*).

That of the left lung passes below the aortic arch and in front of the descending aorta (Goerres et al., 2002). The vertical sequence at the left hilum is pulmonary artery, principal bronchus, and lower pulmonary vein (David et al., 2005).

There are two lobes on the left: the upper and lower, separated by the major (oblique) fissure; and three on the right: the upper, middle and lower lobes separated by the major (oblique) and minor (horizontal) fissures. The fissures are frequently incomplete (Simon et al., 2008).

The right oblique fissure separates the inferior from the middle and upper lobes, and corresponds closely to the left oblique fissure, although it is less vertical, and crosses the inferior border of the lung 7.5 cm behind its anterior end. On the posterior border it is either level with the spine of the fourth thoracic vertebra or slightly lower (*David et al.*, 2005).

The right short horizontal fissure separates the superior and middle lobes. It passes from the oblique fissure, near the mid-axillary line, horizontally forwards to the anterior border of the lung, level with the sternal end of the fourth costal cartilage and then passes backwards to the hilum on the mediastinal surface (*David et al.*, 2005).

The left oblique fissure begins on the medial surface at the posterosuperior part of the hilum. It ascends obliquely backwards to cross the posterior border of the lung 6 cm below the apex, and then descends forwards across the costal surface, to reach the lower border almost at its anterior end. It finally ascends on the medial surface to the lower part of the hilum. A left horizontal fissure is a normal variant found in 10% of patients (*David et al.*, 2005).

In 1% of the population an accessory fissure called the 'azygos fissure' is seen. This fissure contains the azygos vein at its lower end and results from failure of normal migration of the azygos vein from the chest wall to its usual position in the tracheobronchial angle and persistence of the invaginated visceral and parietal pleurae. This fissure may be smaller and therefore less transradiant than corresponding normal lung (Simon et al., 2008).

Other accessory fissures are occasionally identified. A minor fissure may separate the lingular segments from the remainder of the upper lobe, similar to the right minor fissure. A horizontally orientated fissure, a superior accessory fissure, may separate the apical segment from the

basal segments of either lower lobe. An inferior accessory fissure is sometimes seen in one or other lower lobe, usually the right, separating the medial and anterior basal segments (Simon et al., 2008).

Tracheobronchial Tree

The tracheobronchial tree constitutes the airway below the vocal cords. The trachea enters the thorax 1-3cm above the level of the suprasternal notch; its intrathoracic portion is 6-9cm in length. In normal human adult males, the tracheal diameter is 1.3-2.5cm in the coronal plane and 1.3-2.7cm in the sagittal plane; in normal human adult females, the tracheal coronal and sagittal diameters are 1-2.1cm and 1-2.3cm, respectively (*Kathryn et al.*, 2008).

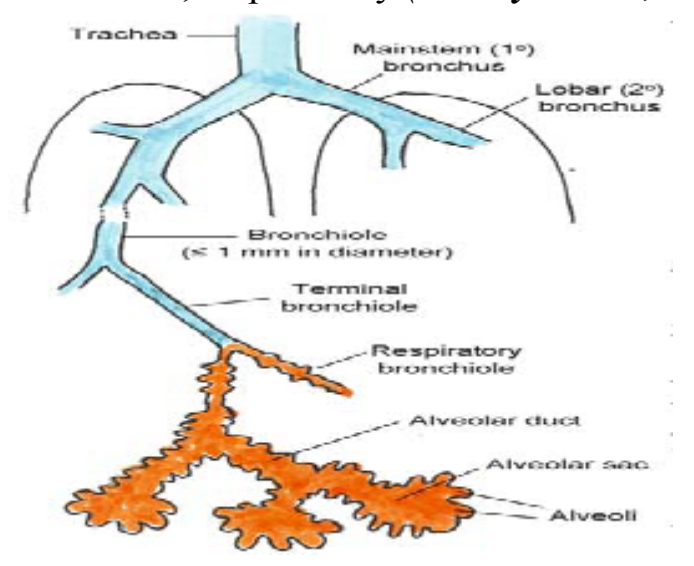


Fig. (4): Schematic demonstration of the tracheobronchial tree (Kathryn et al., 2008).